

Solid State Photochemistry of Novel Composites Containing Luminescent Metal Centers and Poly(2-methoxyaniline-5-sulfonic acid)

Lynn Dennany,^{*,†,‡} Emmet J. O'Reilly,[‡] Peter C. Innis,[†] Gordon G. Wallace,[†] and Robert J. Forster[‡]

Intelligent Polymer Research Institute and ARC Centre of Excellence for Electromaterials Science, AIIM Facility, Innovation Campus, University of Wollongong, Fairy Meadow, NSW 2519, Australia, and Biomedical Diagnostics Institute, National Centre for Sensor Research, School of Chemical Sciences, Dublin City University, Dublin 9, Ireland

Received: February 27, 2009; Revised Manuscript Received: April 6, 2009

Steady state luminescence and measurements of the luminescent lifetime as well as cyclic voltammetry have been used to elucidate the mechanism and dynamics of interaction between a luminescent ruthenium metal center and two different fractions of poly(2-methoxyaniline-5-sulfonic acid) (PMAS). The two fractions, high molecular weight (HMWT) PMAS and low molecular weight (LMWT) PMAS oligomer, showed significantly distinctive influences on the luminophore. The HMWT PMAS, confirmed to be an emeraldine salt by its characteristic redox chemistry, greatly impacted the diffusion coefficient of the $\text{Ru}^{2+/3+}$ within the composite film, increasing the diffusion coefficient, D_{CT} , by 2 orders of magnitude. The HMWT PMAS also resulted in quenching of the ruthenium-based emission. Significantly, these results indicate that quenching involves both static and dynamic processes, with the static quenching being the dominant process, suggesting that the metal center and polymer backbone were strongly associated. In stark contrast, the LMWT PMAS did not influence the electrochemical properties of the ruthenium metal center; however, it did double the emission observed from the ruthenium metal center. The insensitivity of the luminescence lifetime does suggest that, as with the HMWT PMAS, LMWT PMAS is strongly associated with the ruthenium metal center. The enhanced luminescence may allow for many potential sensor developments based on the luminescent ruthenium metal center, while the HMWT PMAS quenching could be utilized within quenching-based strategies or electrochemical devices.

Introduction

The use of polymers as supports for confining transition metals at the electrode–solution interface is well-known.^{1,2} The subsequent interaction of an inherently conducting polymer and a luminescent metal center to produce novel materials has been an attractive approach to forming interfacial metallopolymer films, since the π conjugated backbone can provide a rapid electron transfer pathway between the metal complex and the electrode.^{1,3–5} In recent times, the possibility of combining an inherently conducting polymer with a metal center has been investigated with a view to taking advantage of electronic communication between metal centers through the conjugated backbone of the polymer.^{6,7} As such, π -conjugated metallopolymer have attracted increased attention because of their potentially widespread applications.^{8,9} The extensive delocalization of π -electrons is known to be responsible for the array of remarkable characteristics that such polymers exhibit.^{1,4,10} These properties include nonlinear optical behavior, electronic conductivity, and exceptional mechanical properties^{11,12} such as tensile strength and resistance to harsh environments. In one study, the extensive delocalization contributed to the substantially enhanced electronic communication between adjacent

metal centers, which allowed for more sensitive sensors to be developed with lower detection limits and faster regeneration times.¹³

Polyelectrolytes incorporating luminescent metal complexes^{6,14,15} are also attractive for spectroscopic-based sensors because of their synthetic flexibility, processability, high absorption coefficients, and relatively high fluorescent quantum yields. In contrast to the “light-producing” transduction strategies, polymers have recently received attention as components in high performance luminescence quenching detection schemes.^{16,17} In this approach, one exploits the luminescent polyelectrolyte's high absorption coefficients in combination with relatively high quantum yields of emission, and the extraordinarily efficient quenching of their luminescence emission by small molecule electron and energy acceptors. In these “super-quenching” or even “hyper-quenching” approaches, a single target molecule can quench more than one luminescent center.¹⁸ Apart from the analytical applications, the demands of achieving artificial photosynthesis have also inspired several studies into the photochemical electron and energy transfer of excited state ruthenium centers in molecular assemblies. Many of these studies highlight the energy migration processes involved in the light harvesting ruthenium “antenna” polymer.

Previous studies have explored the incorporation of a ruthenium metal center by ion pairing with sulfonate groups of poly(2-methoxyaniline-5-sulfonic acid) (PMAS).^{13,19} These novel composites exhibited enhanced electronic communication between adjacent metal centers as well as modulated photophysical properties.^{13,19} However, the improvements in response time and

* Corresponding author. Phone: +61 2 4298 1428. Fax: +61 2 4298 1499. E-mail: lynnnd@uow.edu.au.

[†] University of Wollongong.

[‡] Dublin City University.

sensitivity for electrochemiluminescence sensing were not as great as expected for this type of conducting polymer. Sulfonated self-doped polyaniline has been extensively studied due to its unique electrochemical properties, water solubility, improved processability, and potential industrial applications.^{20–22} PMAS is a fully sulfonated conducting polymer that has been synthesized by chemical and electrochemical polymerization of 2-methoxyaniline-5-sulfonic acid (MAS).^{23,24}

Electrochemical synthesis produces PMAS, which has been shown to contain two distinct polymer fractions with molecular weights of approximately 8–10 and 2 kDa, respectively.^{25,26} It has been found that upon separation these two fractions of PMAS exhibit distinctly different electrochemical and photochemical properties.²⁶ The high molecular weight (HMWT) PMAS (M_w of 8–10 kDa) was confirmed to be an emeraldine salt by its characteristic redox and pH switching behavior but showed no photoluminescence. In contrast, the low molecular weight (LMWT) PMAS (M_w of ca. 2 kDa) was shown to be electrochemically inert but exhibited intense photoluminescence. Innis et al. have examined the differences between these two fractions in detail.^{20,26,27}

Since it is now possible to isolate these polymer fractions, their individual interactions with a ruthenium metal center can be investigated. The opposing electrochemical and photochemical properties of the individual PMAS fractions should have very distinct influences on the ruthenium metal center, thereby enabling improvements in sensor response by tailoring of the sensor design to a specific application based on enhanced electronic communication or enhanced/quenched luminescence.

In this contribution, we report on the individual influences of the two fractions of PMAS on the photophysical properties of a luminescent metal center. Steady state luminescence and measurements of luminescent lifetimes have been utilized to elucidate the influence of these fractions. Significantly, the two fractions show opposing effects on the photochemical properties of $\text{Ru}^{2+/3+}$. The LMWT PMAS was shown to enhance the observed ruthenium-based emission, while the HMWT PMAS was shown to effectively quench the ruthenium emission via a static resonant energy transfer. By utilizing the individual fractions of PMAS, different energy and electron transfer mechanisms can occur between the ruthenium metal center and the polymer backbone. This would modulate the photochemical properties of the ruthenium for the desired purpose, be that as a luminescent or quenching sensor or an electrochemically based detection system.

Experimental Section

Apparatus. Absorbance and photoluminescence were recorded using a Shimadzu UV-240 spectrophotometer and a JY Spex fluorescence spectrophotometer, respectively. An ITO modified electrode was used as the working electrode with platinum flag and Ag/AgCl electrode acting as counter and reference electrodes, respectively. Potentials are quoted versus Ag/AgCl, and all measurements were made at room temperature.

Fluorescence lifetime studies were made on a PicoQuant PDL-800B pulsed diode laser controller and FluoTime 100 time-correlated single photon counting (TCSPC) system with 280, 370, and 450 nm pulsed laser sources with cut-on filters of 400, 475, and 530 nm. TCSPC analysis was performed using PicoQuant FluoFit software. Samples were deoxygenated for approximately 20 min with nitrogen prior to analysis. ITO conductive glass was obtained from Hartford Glass Co. Inc. (Hartford City, IN) and was cut into 0.8×2 cm working electrodes. These electrodes were utilized for all spectrochemical

analysis. First, the working electrodes were rinsed with ethanol and gradually heated to 400 °C for 15 min, and then, they were cleaned with household detergent in water, then deionized water, followed by acetone, and finally deionized water. The electrodes were then dried completely under a flow of nitrogen gas and modified with the Ru–PMAS composite prior to use. Solutions were purged with pure nitrogen for 15 min prior to each series of experiments, and a nitrogen atmosphere was maintained during data collection.

Materials and Reagents. $[\text{Ru}(\text{bpy})_3]^{2+}$ was purchased from Sigma Aldrich as its chloride salt and used as received. Poly(acrylic acid) (PAA) 50 wt % solution in water was purchased from Sigma Aldrich and used as received. PMAS emeraldine salt was prepared via the chemical synthesis method and then fractionated using a recently described cross-floss dialysis.²⁸ The two pure fractions were labeled high molecular weight (HMWT) PMAS (8–10 kDa) and low molecular weight (LMWT) PMAS (2 kDa). All other reagents used were of analytical grade, and all solutions were prepared in Milli-Q water (18 mΩcm).

Composite Synthesis. Composite solutions containing $[\text{Ru}(\text{bpy})_3]^{2+}$ and either HMWT or LMWT PMAS in ethanol were prepared. Where appropriate, working electrodes were modified by applying a drop ($\approx 200 \mu\text{L}$) of an ethanolic solution of the composite to the electrode surface (0.1–1.0% depending on the desired surface coverage) and dried in the dark for 10–12 h. These modified electrodes were then washed (Milli-Q water) and allowed to dry overnight prior to analysis. Post-synthesis characterization was performed in aqueous 0.1 M H_2SO_4 unless otherwise stated. The surface coverages of the composite films, Γ , were determined by graphical integration of background corrected cyclic voltammograms ($<5 \text{ mV s}^{-1}$). The surface coverage for all composite films was approximately $(7 \pm 2) \times 10^{-9} \text{ mol cm}^{-2}$ unless otherwise stated. The resulting electrodeposited films were sparingly soluble in water due to the Ru complex cation ionically cross-linking the water-soluble PMAS polymer via the “free” sulfonic acid substituent. For comparison purposes, $[\text{Ru}(\text{bpy})_3]^{2+}$ was also dissolved in PAA 50 wt % solution in H_2O and $\sim 200 \mu\text{L}$ was cast onto an ITO electrode.

Results and Discussion

Steady State Luminescence of Composites. Previous fluorescence studies on Ru–PMAS composites were carried out on an electrochemically grown composite film. UV–vis spectral studies showed that the composition of the PMAS present in the film contained approximately 70% w/v HMWT PMAS and 30% w/v LMWT PMAS.^{26,28} This type of film resulted in a reduced ruthenium-based luminescence when compared to films containing a nonconducting polymer, such as poly(4-vinylpyridine) (PVP), when excited at 355 nm. This reduction was attributed to a simple quenching of the ruthenium metal center by absorption of the PMAS present in the film. However, given the opposing photochemical properties of the two fractions of PMAS, it is unlikely that both quench the ruthenium metal center to the same extent or by the same mechanisms. The influence on the luminescence of ruthenium metal centers by the pure HMWT PMAS emeraldine salt and its oligomer LMWT PMAS fraction is examined in this contribution. The luminescence of the ruthenium bipyridyl complex is shown to be efficiently quenched by the HMWT PMAS emeraldine salt, whereas ruthenium-based emission is enhanced when the metal interacts with the LMWT PMAS fraction. Figure 1 illustrates the effects on the ruthenium-based emission on solid state samples with increasing HMWT or LMWT PMAS.

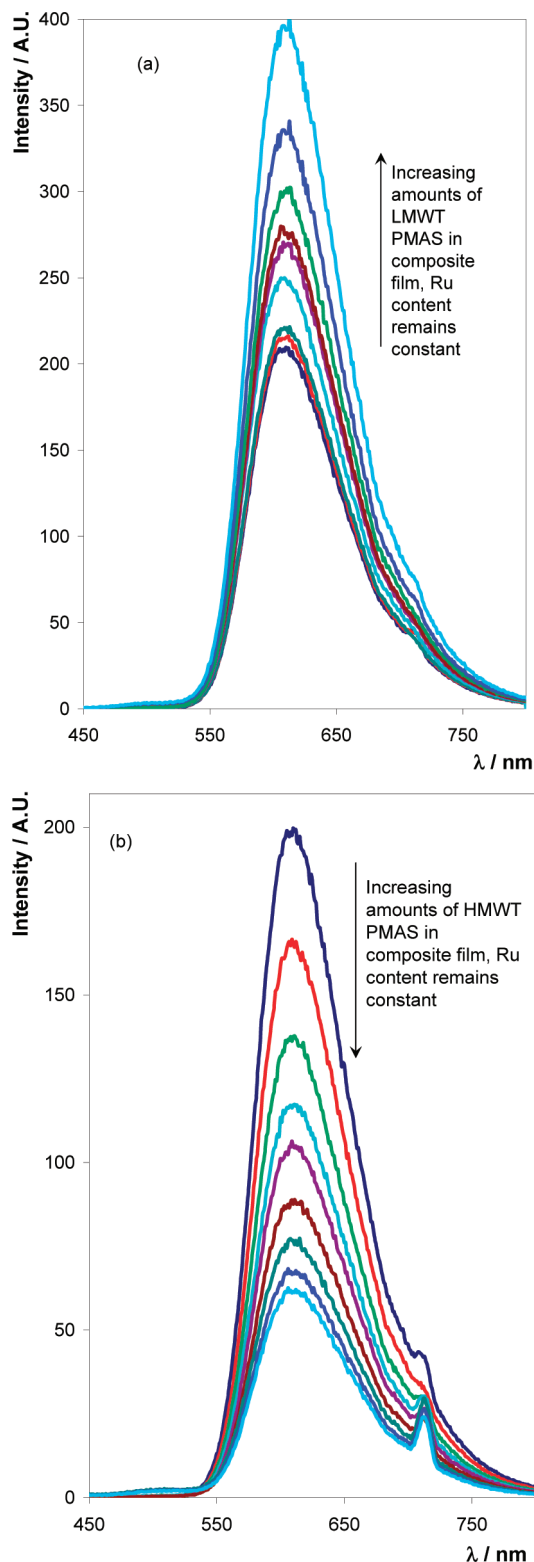


Figure 1. Typical solid state luminescence spectra for composite films of (a) Ru-HMWT PMAS and (b) Ru-LMWT PMAS on ITO electrodes with increasing amounts of (a) LMWT PMAS and (b) HMWT PMAS while maintaining a constant $[\text{Ru}^{2+}]$.

Quenching may arise from a number of different processes. For example, “dynamic” quenching involves a collisional encounter between the quencher and the excited state resulting in the lifetime and intensity of the emission both decreasing. Alternatively, “static” quenching arises where an interaction between the luminophore and quencher exists in the ground state. Pure static quenching can be identified, since it reduces

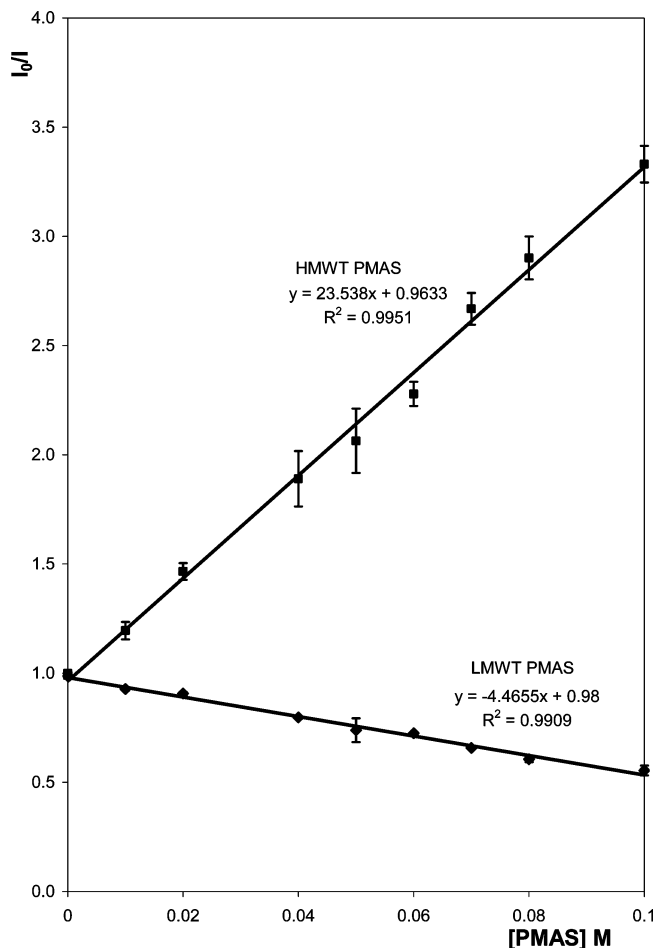


Figure 2. Stern–Volmer plots for the Ru–PMAS composite films ($\Gamma = (6.7 \pm 2) \times 10^{-9} \text{ mol cm}^{-2}$) based on the steady state emission intensity data in Figure 1.

the luminescence intensity but does not generally decrease the measured lifetime of emission. Dynamic quenching can be modeled using the Stern–Volmer equation:

$$I_0/I = \tau_0/\tau = 1 + k_q\tau_0[Q] \quad (1)$$

where I_0 and I are the luminescence intensities in the absence and presence of quencher, respectively, k_q is the collision quenching rate, τ_0 is the luminescence lifetime without any quencher present, and $[Q]$ is the concentration of the quencher, HMWT PMAS.

It is important to note that the emission intensities must be corrected for the absorbance of the quencher at the exciting wavelength and therefore absorbance corrections were made using standard procedures.^{29,30} If the luminophore can form a stable complex with a quenching molecule, the resultant ground state of the luminophore–quencher complex is said to be statically quenched. In this case, the Stern–Volmer equation is modified, where $k_q\tau_0$ can be substituted by K_{SV} , the Stern–Volmer constant.

The Stern–Volmer plot for the quenching of the ruthenium metal center by HMWT PMAS is shown in Figure 2. This plot indicates that HMWT PMAS effectively quenches the ruthenium-based emission. The Stern–Volmer equation is normally utilized to describe solution phase systems with diffusion controlled collision events. Such processes are clearly not present in these solid state materials, where the $\text{Ru}^{2+/3+}$ centers are ionically bound to the PMAS SO_3^- functionalities. It is well-known that photoluminescence quenching in conducting polymer systems

originates from the presence of polaronic (radical cation) charge carriers.^{31–34} It is also known that these polaronic species possess a high degree of inter- and intrachain mobility. It is therefore the presence of the mobile polaronic quenchers in the PMAS polymer the Stern–Volmer model finds application.

This quenching also highlights the rationale for poor luminescence previously observed for the electrochemically grown Ru–PMAS composite films, which as stated above contained approximately 70% w/v HMWT PMAS. The influence of the LMWT PMAS fraction on the luminescence of $[\text{Ru}(\text{bpy})_3]^{2+}$ is illustrated in Figure 1a and the subsequent Stern–Volmer plot in Figure 2. In sharp contrast to its oligomer, HMWT PMAS, the LMWT fraction resulted in an enhanced ruthenium-based emission. This enhancement is most likely due to an energy transfer from the emissive LMWT PMAS fraction to the ruthenium metal center. In effect, there is energy transfer from the LMWT PMAS to the $[\text{Ru}(\text{bpy})_3]^{2+}$ and it is this energy transfer from the LMWT PMAS that results in an enhancement of the ruthenium emission.

Luminescence Lifetimes of Composites. The luminescent lifetime can provide useful insights into the mechanism of excited state energy transfer between the metal center and the quencher. A time-correlated single photon counting (TCSPC) system was employed using 370 nm pulsed laser sources. A cut-on filter of 400 nm was also utilized. Typical TCSPC responses for Ru–HMWT PMAS and Ru–LMWT PMAS are shown in Figure 3. In each instance, the trace relates to the TCSPC output and the resultant model fit. The TCSPC responses in each case were collected to the same photon count intensity (10 000 counts). Emission responses were analyzed using PicoQuant FluoFit software employing a fitting function containing two time constants.

$[\text{Ru}(\text{bpy})_3]^{2+}$ typically exhibits a single exponential decay in solution of 680 ± 18 ns. When incorporated into a PVA film, a nonreactive polymer, $[\text{Ru}(\text{bpy})_3]^{2+}$, exhibits a multiexponential decay in the solid state. The luminescent decay of the solid state $[\text{Ru}(\text{bpy})_3]^{2+}$ is characterized by short- and long-lived components that have lifetimes of 506 ± 8 ns (population fraction 0.8) and 150 ± 6 ns (population fraction 0.2), respectively (see the Supporting Information). The composite films exhibit a more complex decay characterized by at least two time constants. Figure 3 confirms that double exponential fits adequately describe the experimental responses. The luminescent decay of the Ru–HMWT PMAS composite film is characterized by short- and long-lived components that have lifetimes of 46 ± 5 ns (population fraction 0.8) and 5 ± 0.2 ns (population fraction 0.2), respectively. The multiexponential behavior may arise from different microenvironments within the film, e.g., poorly solvated or cross-linked chains that increase the rigidity of the complex and decrease the rate of vibrational relaxation.³⁵ The short time scale decay becomes increasingly significant with an increasing concentration of the quencher within the film, as is evident in Figure 3. The lifetime of the dominant component in the presence of the quencher is taken as τ and clearly indicates that the presence of HMWT PMAS within the film causes the luminescence intensity and lifetime to decrease, suggesting dynamic quenching processes.

A typical Stern–Volmer plot for luminescence lifetime, τ_0/τ versus $[\text{Q}]$, is shown in Figure 3. When luminescence quenching occurs solely by dynamic quenching, the slopes of plots of I_0/I and τ_0/τ should be identical and the Stern–Volmer constant, K_{SV} , is equal to k_q . Figure 3 shows that the slopes of the τ_0/τ and Stern–Volmer plots are 7.1 ± 0.6 and 23.5 ± 2.1 , respectively. The fact that these slopes differ from one another

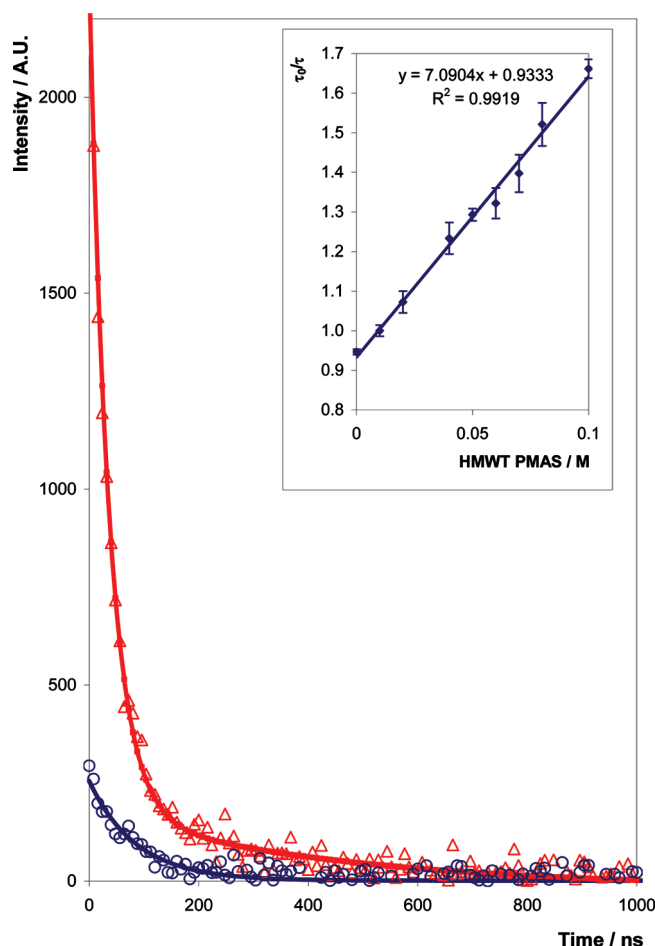


Figure 3. Typical transient emission spectra for thin films of (a) Ru–HMWT PMAS (blue line) and (b) Ru–LMWT PMAS (red line) on ITO electrodes. An excitation wavelength of 370 nm was utilized. Photon counts of 10 000 were utilized. The inset shows the Stern–Volmer plot for the Ru–HMWT PMAS composite films based on luminescent lifetime data. The surface coverage for all composite films was approximately $(6.7 \pm 2) \times 10^{-9}$ mol cm^{-2} .

indicates that while dynamic quenching occurs in this system to an extent, it does not fully account for the decrease in emission observed in the presence of the HMWT PMAS fraction. Therefore, it appears that some of the luminophores can physically move within the lifetime of the excited state, giving rise to a dynamic quenching contribution, but that static quenching represents the most significant quenching mechanism. This conclusion appears reasonable given that the luminophores and quenchers are both confined to the electrode surface and physical displacement will involve at least segmental polymer chain movement of the PMAS. Moreover, this conclusion is entirely consistent with ground state measurements of the rate of homogeneous charge transport that show that the redox centers have significant mobility.

The luminescence lifetime of the Ru component of the Ru–LMWT PMAS composites is independent of LMWT PMAS concentration. The luminescent decay of the Ru–LMWT PMAS composite film is also characterized by short- and long-lived components that have lifetimes of 427 ± 15 ns (population fraction 0.7) and 36 ± 5 ns (population fraction 0.3), respectively, which remain constant with increasing concentrations of the LMWT PMAS within the composite film containing a constant Ru concentration. Therefore, although the LMWT PMAS enhances the emission of the ruthenium metal center, there is not a very strong influence on the excited state lifetime.

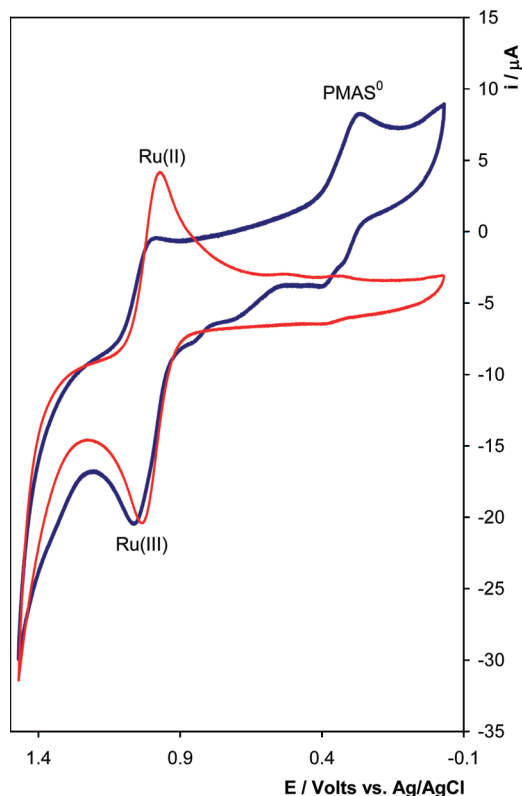


Figure 4. Typical cyclic voltammograms of thin films of (red) Ru-LMWT PMAS and (blue) Ru-HMWT PMAS following film formation on ITO electrodes. The electrolyte was 0.1 M H₂SO₄, and a scan rate of 100 mV s⁻¹ was used. The surface coverage for both was $(6.7 \pm 2) \times 10^{-9}$ mol cm⁻². Cyclic voltammograms were recorded over the range $-0.1 \leq E$ (volts) ≤ 1.4 with the CV starting at -0.1 V.

The presence of the short lifetime component is attributed to small amounts of HMWT PMAS impurities within the composite film and to the fact that the film structure may not be homogeneous, leading to a nonuniform distribution of luminophores throughout the film. This may lead to reductions in the electrostatic repulsions between the luminophores, increasing the likelihood of self-quenching and resulting in different microenvironments which allow the alternatives in the relaxation processes occurring in the composite film. This would be observed in a multiexponential decay process. The fact that the lifetime of the ruthenium metal center remains unchanged by increasing the LMWT PMAS concentration within the composite suggests that they associate strongly in the ground state.

Electrochemical Properties of the Novel [Ru(bpy)₃]²⁺-PMAS Composites. Figure 4 shows the typical cyclic voltammograms obtained for composite films of the two different Ru-PMAS following composite film formation versus Ag/AgCl. The voltammetric behavior of PMAS has been reported previously,²⁸ as has the voltammetric behavior of the electrochemically grown Ru-PMAS composite films.^{36,37} Surface coverage, Γ , for the composite films utilized in this study was calculated by graphical integration of background corrected peaks associated with the Ru^{2+/3+} process at approximately 1.1 V using slow scan rates (<5 mV s⁻¹).³⁸ For both Ru-PMAS composites, Γ was $(6.9 \pm 4.2) \times 10^{-9}$ mol cm⁻². The formal potential of the Ru^{2+/3+} couple and the typical anodic and cathodic behavior, which were attributed to leucoemeraldine to emeraldine and emeraldine to pernigraniline redox transitions, respectively, can be seen for the Ru-HMWT PMAS composite, while only the Ru^{2+/3+} couple was observed for the Ru-LMWT

TABLE 1: Typical Formal Potentials and Diffusion Coefficients, D_{ct} , of the Various Ruthenium PMAS Composite Films Used during This Study

composite	D_{ct}^a (cm ² s ⁻¹)	$E^0(\text{Ru}^{2+/3+})$ (V) vs Ag/AgCl ^b
Ru-PMAS ^c	3.11×10^{-10}	1.02
Ru-HMWT PMAS	4.48×10^{-9}	1.04
Ru-LMWT PMAS	1.73×10^{-11}	1.01

^a D_{ct} represents the diffusion coefficient of these composite films.

^b 0.1 M H₂SO₄ was used as the supporting electrolyte. ^c Electrochemically grown Ru-PMAS composite film, values taken from ref 13.

PMAS. The electrochemical behavior of both the metal center and the conducting polymer were consistent with previous studies on the electrochemically grown Ru-PMAS composite films that contained a mixture of both HMWT and LMWT PMAS.

Table 1 contains the charge transfer diffusion coefficient, D_{ct} , values for the PMAS composites and the electrochemically grown Ru-PMAS film from previous studies.¹³ This table shows that the diffusion coefficient calculated for the ruthenium redox couple with the HMWT PMAS composite is approximately an order of magnitude larger ($(4.5 \pm 0.9) \times 10^{-9}$ cm² s⁻¹) than that found for the previously studied system ($(3.1 \pm 0.8) \times 10^{-10}$ cm² s⁻¹). In contrast, the LMWT PMAS does not enhance the diffusion coefficient, being comparable to systems containing a nonconducting polymer backbone such as PVP. These results illustrate that the HMWT PMAS supports more rapid charge propagation between the ruthenium metal centers within the composite compared to both the Ru-LMWT PMAS composites and a nonconducting polymer system.

Conclusions

By isolating the two fractions of the conducting polymer, poly(2-methoxyaniline-5-sulfonic acid) (PMAS), the photochemical properties of novel composites with [Ru(bpy)₃]²⁺ can be modulated. Significantly, the oligomeric LMWT PMAS fraction is known to exhibit photoluminescence and its subsequent association with [Ru(bpy)₃]²⁺ is shown to enhance the luminescence from the Ru^{2+/3+} metal center without affecting the excited state lifetime of the metal center. In contrast, the pure HMWT PMAS emeraldine salt is shown to quench the luminescence of the [Ru(bpy)₃]²⁺ predominantly by a static quenching mechanism.

However, spectrochemical and electrochemical analysis reveals that the HMWT PMAS emeraldine salt supports a more rapid electron transfer within the film, increasing the D_{CT} values by 2 orders of magnitude compared to the Ru-LMWT PMAS composite which does not affect the electrochemical behavior of the ruthenium metal center. Therefore, this contribution illustrates that both the photochemical and electrochemical properties of the luminescent metal center can be modulated to enhance either the photoluminescence or the charge transfer by interacting with either the LMWT or HMWT PMAS. This may allow for each fraction to be utilized in very different applications depending on the desired function. These findings demonstrate the many possible applications for which these composites can be exploited for, including luminescence- and quenching-based sensors.

Acknowledgment. The financial support of Science Foundation Ireland under the Biomedical Diagnostics Institute (Award No. 05/CE3/B754) is deeply appreciated. The continued financial support from the Australian Research Council under the

Centers of Excellence and QE(II) Fellowship (P.C.I.) programs and through the Australian Research Council Nanotechnology Network (L.D.) is also greatly appreciated.

Supporting Information Available: Figure showing the luminescent decay of $[\text{Ru}(\text{bpy})_3]^{2+}$ in the solid state. This material is available free of charge via the Internet at <http://pubs.acs.org>.

References and Notes

- (1) Pickup, P. G. *J. Mater. Chem.* **1999**, 9, 1641–1653.
- (2) Cosnier, S. *Biosens. Bioelectron.* **1999**, 14, 443–456.
- (3) Ochmanska, J.; Pickup, P. G. *J. Electroanal. Chem.* **1989**, 271, 83–105.
- (4) Cameron, C. G.; Pickup, P. G. *Chem. Commun.* **1997**, 3, 303–304.
- (5) Cameron, C. G.; Pickup, P. G. *J. Am. Chem. Soc.* **1999**, 121, 7710–7711.
- (6) Forster, R. J.; Vos, J. G. *J. Chem. Soc., Faraday Trans.* **1991**, 87, 1863–1867.
- (7) Cameron, C. G.; Pickup, P. G. *J. Am. Chem. Soc.* **1999**, 121, 11773–11779.
- (8) Arnold, F. E. J.; Arnold, F. E. *Adv. Polym. Sci.* **1994**, 117, 257.
- (9) Vogel, H.; Marvel, C. S. *J. Polym. Sci.* **1961**, L, 511.
- (10) Ochmanska, J.; Pickup, P. G. *J. Electroanal. Chem.* **1989**, 271, 83–105.
- (11) Osaheni, J. A.; Jenekhe, S. A. *Chem. Mater.* **1992**, 4, 1282.
- (12) Roberts, M. F.; Jenekhe, S. A. *Chem. Mater.* **1994**, 6, 135.
- (13) Dennany, L.; O'Reilly, E. J.; Innis, P. C.; Wallace, G. G.; Forster, R. J. *Electrochim. Acta* **2008**, 53, 4599–4605.
- (14) Doherty, A. P.; Forster, R. J.; Smyth, M. R.; Vos, J. G. *Anal. Chim. Acta* **1991**, 255, 45–52.
- (15) Lyons, C. H.; Abbas, E. D.; Lee, J.-K.; Rubner, M. F. *J. Am. Chem. Soc.* **1998**, 120, 12100.
- (16) Li, C.-Y.; Zhang, X.-B.; Jin, Z.; Han, R.; Shen, G.-L.; Yu, R.-Q. *Anal. Chim. Acta* **2006**, 580, 143–148.
- (17) Fleming, C. N.; Maxwell, K. A.; DeSimone, J. M.; Meyer, T. J.; Papanikolas, J. M. *J. Am. Chem. Soc.* **2001**, 123, 10336–10347.
- (18) Kwon, S.; Carson, J. H. *Anal. Biochem.* **1998**, 264, 133–140.
- (19) Dennany, L.; Innis, P. C.; Wallace, G. G.; Forster, R. J. *J. Phys. Chem. B* **2008**, 112, 12907–12912.
- (20) Zhou, D.; Innis, P. C.; Wallace, G. G.; Shimizu, S.; Maeda, S.-I. *Synth. Met.* **2000**, 114, 287–293.
- (21) Shimizu, S.; Saitoh, T.; Uzawa, M.; Yuasa, M.; Yano, K.; Maruyama, T.; Watanabe, K. *Synth. Met.* **1997**, 85, 1337–1338.
- (22) Wei, X.-L.; Wang, Y. Z.; Long, S. M.; Bobeczko, C.; Epstein, A. J. *J. Am. Chem. Soc.* **1996**, 118, 2545–2555.
- (23) Masdarolomoor, F.; Innis, P. C.; Ashraf, S.; Wallace, G. G. ICSM 2004, Wollongong, Australia, 2004.
- (24) Masdarolomoor, F.; Innis, P. C.; Ashraf, S.; Wallace, G. G. *Synth. Met.* **2005**, 153, 181–184.
- (25) Masdarolomoor, F.; Innis, P. C.; Ashraf, S.; Kaner, R. B.; Wallace, G. G. *Macromol. Rapid Commun.* **2006**, 27, 1995–2000.
- (26) Innis, P. C.; Masdarolomoor, F.; Kane-Maguire, L. A. P.; Forster, R. J.; Keyes, T. E.; Wallace, G. G. *J. Phys. Chem. B* **2007**, 111, 12738–12747.
- (27) Guo, R.; Barisci, J. N.; Innis, P. C.; Too, C. O.; Wallace, G. G.; Zhou, D. *Synth. Met.* **2000**, 114, 267–272.
- (28) Masdarolomoor, F.; Innis, P. C.; Ashraf, S.; Wallace, G. G. *Synth. Met.* **2005**, 153, 181–184.
- (29) Demas, J. N.; Adamson, A. W. *J. Am. Chem. Soc.* **1973**, 95, 5159–5168.
- (30) Navon, G.; Sutin, N. *Inorg. Chem.* **1974**, 13, 2159–2164.
- (31) Karpacheva, G. P.; Orlov, A. V.; Rykov, S. V.; Skakovsky, E. D. *ANTEC* **1992**, 56.
- (32) Son, Y.; Patterson, H. H.; Carlin, C. M. *Chem. Lett. Phys.* **1989**, 162, 461.
- (33) Asberg, P.; Nilsson, P.; Inganas, O. *J. Appl. Phys.* **2004**, 96, 3140.
- (34) Lee, S.; Lee, J. Y.; Lee, H. *Synth. Met.* **1999**, 101, 248.
- (35) Dennany, L.; Hogan, C. F.; Keyes, T. E.; Forster, R. J. *Anal. Chem.* **2006**, 78, 1412–1417.
- (36) Dennany, L.; Forster, R. J.; Rusling, J. F. *J. Am. Chem. Soc.* **2003**, 125, 5213–5218.
- (37) Dennany, L.; Forster, R. J.; White, B.; Smyth, M.; Rusling, J. F. *J. Am. Chem. Soc.* **2004**, 126, 8835–8841.
- (38) Tokel, N. E.; Bard, A. J. *J. Am. Chem. Soc.* **1972**, 94, 2862–2863.

JP901808D